

Observational and Modeling Constraints on Global Anthropogenic Enrichment of Mercury

Helen M. Amos,^{*,†} Jeroen E. Sonke,[‡] Daniel Obrist,[§] Nicholas Robins,^{||} Nicole Hagan,[⊥] Hannah M. Horowitz,[#] Robert P. Mason,[∇] Melanie Witt,[○] Ian M. Hedgecock,[◆] Elizabeth S. Corbitt,[#] and Elsie M. Sunderland^{†,¶}

[†]Department of Environmental Health, Harvard T. H. Chan School of Public Health, Boston, Massachusetts 02115, United States

[‡]Laboratoire Géosciences Environnement Toulouse, Observatoire Midi-Pyrénées, CNRS-IRD-Université Paul Sabatier, 31062 Toulouse, France

[§]Desert Research Institute, Reno, Nevada 89512, United States

^{||}Department of History, North Carolina State University, Raleigh, North Carolina 27695, United States

[⊥]Environmental Health Council, Durham, North Carolina 27701, United States

[#]Department of Earth and Planetary Sciences, Harvard University, Cambridge, Massachusetts 02138, United States

[∇]Department of Marine Sciences, University of Connecticut, Groton, Connecticut 06340, United States

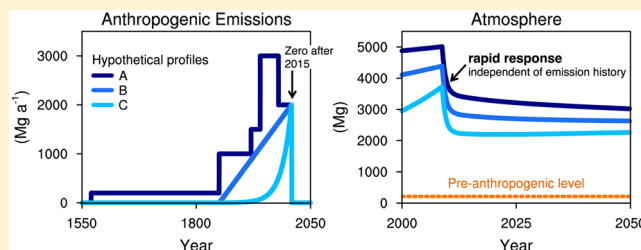
[○]Department of Physiology, Anatomy and Genetics, University of Oxford, Oxford OX1 3QX, United Kingdom

[◆]Rende Division, CNR-Institute of Atmospheric Pollution Research, 87036 Rende, Italy

[¶]School of Engineering and Applied Sciences, Harvard University, Cambridge, Massachusetts 02138, United States

Supporting Information

ABSTRACT: Centuries of anthropogenic releases have resulted in a global legacy of mercury (Hg) contamination. Here we use a global model to quantify the impact of uncertainty in Hg atmospheric emissions and cycling on anthropogenic enrichment and discuss implications for future Hg levels. The plausibility of sensitivity simulations is evaluated against multiple independent lines of observation, including natural archives and direct measurements of present-day environmental Hg concentrations. It has been previously reported that pre-industrial enrichment recorded in sediment and peat disagree by more than a factor of 10. We find this difference is largely erroneous and caused by comparing peat and sediment against different reference time periods. After correcting this inconsistency, median enrichment in Hg accumulation since pre-industrial 1760 to 1880 is a factor of 4.3 for peat and 3.0 for sediment. Pre-industrial accumulation in peat and sediment is a factor of ~5 greater than the precolonial era (3000 BC to 1550 AD). Model scenarios that omit atmospheric emissions of Hg from early mining are inconsistent with observational constraints on the present-day atmospheric, oceanic, and soil Hg reservoirs, as well as the magnitude of enrichment in archives. Future reductions in anthropogenic emissions will initiate a decline in atmospheric concentrations within 1 year, but stabilization of subsurface and deep ocean Hg levels requires aggressive controls. These findings are robust to the ranges of uncertainty in past emissions and Hg cycling.



1.0. INTRODUCTION

Humans have been releasing mercury (Hg) to the environment since antiquity, resulting in accumulation of anthropogenic Hg in the ocean, atmosphere, and terrestrial ecosystems. Much of the anthropogenic Hg deposited to terrestrial and aquatic ecosystems is re-emitted to the atmosphere, prolonging its residence time in the environment.¹ The ultimate fate of this anthropogenic perturbation is sequestration in sediment,² primarily in the coastal zone.³ Here we refer to the re-emitted component of anthropogenic Hg as “legacy” Hg. We define “natural” Hg as that originating from geogenic sources. This includes primary releases (e.g., volcanism and weathering) and

re-emission of geogenically derived Hg from soils and the ocean to the atmosphere. Ecosystem responses to reductions in anthropogenic emissions, such as those targeted by the Minamata Convention, are affected by the magnitude and timing of legacy re-emissions from environmental reservoirs. Here we review available evidence for accumulation of legacy Hg in global environmental reservoirs, quantitatively discuss

Received: December 3, 2014

Revised: March 6, 2015

Accepted: March 9, 2015

Published: March 9, 2015

Table 1. Description of Model Sensitivity Simulations

scenario numbers	short name	description of changes made relative to Amos et al. ³ model
1	mining decreased 3×	forced by Streets et al. ¹⁹ inventory with 1570-to-1920 large-scale Hg, Ag, and Au mining emissions decreased by a factor of 3 as in Zhang et al. ³²
2	zero pre-1850 emissions	forced by Streets et al. ¹⁹ inventory with 1850-to-1920 large-scale Hg, Ag, and Au mining emissions decreased by 50% and zero pre-1850 emissions
3	greater geogenic emissions	increase geogenic emissions from 76 to 300 Mg year ⁻¹
4	increased ocean evasion	increase the rate coefficient for ocean evasion by +30%
5	greater soil retention	decrease the rate coefficients for Hg(0) evasion from the slow and armored organic soil reservoirs by a factor of 5
6	greater burial	90% of total particle-bound Hg discharged by rivers buried in benthic sediment at ocean margins

The time history of emission scenarios 1 and 2 are shown in SI Figure S1.

uncertainties in the global Hg budget, and analyze implications for future environmental responses.

Information on historical Hg accumulation can be drawn from multiple natural archives, including aquatic sediment, ombrotrophic peat, glacial ice, and biological tissues.^{4–8} Lake sediment and peat archives are commonly used to indicate changes in Hg accumulation. Each archive reflects different time intervals of accumulation and can be disturbed by a variety of postdepositional processes.^{9,10} In both cases, careful selection of sampling sites and analysis of evidence for disturbance by investigators establishes reliability as an indicator of historical pollution.¹¹

Remote lake sediments have been widely reported to converge around a 3-fold increase in Hg accumulation in the modern era relative to the pre-industrial (1850) period after correcting for sediment focusing, watershed inputs, and other factors.^{12–14} Prior work reported a 40-fold pre-industrial to present increase in peat Hg accumulation rates,¹⁵ but we find the temporal periods of accumulation being compared were not the same. This has artificially inflated the apparent discrepancy across archives, and we correct for this here to revisit the comparison of Hg accumulation in remote lake sediment and peat records.

Global biogeochemical Hg models extend observations in space and time and provide complementary information to natural archives of Hg accumulation. The first generation of models prescribed a factor of 3 pre-industrial-to-present enrichment of atmospheric deposition to estimate Hg accumulation in the ocean and terrestrial ecosystems.^{1,16–18} Recently, the availability of historical inventories of global anthropogenic Hg releases^{19,20} and accounting for longer time scales of coupling among the atmosphere, terrestrial ecosystems, and the ocean have allowed an independent, alternate method for characterizing the global Hg cycle.^{3,21}

Multiple historical inventories of atmospheric Hg emissions^{19,22–25} point to substantial pre-1850 and late 19th century Hg emissions to the atmosphere associated with the massive quantities of Hg consumed for early gold and silver mining activities.^{24,26–28} The proportion of Hg released to the atmosphere during pre-1850 and late 19th century mining activities and the spatial extent of these impacts is a subject of ongoing debate. Some recent work suggests releases to the atmosphere are only a small fraction of the total Hg consumed^{13,29} and impacts are restricted to the local environment.^{30,31}

The objective of this review is to bracket plausible scenarios for global anthropogenic enrichment of Hg based on current estimates of primary emissions and rates of exchange between environmental reservoirs. Global anthropogenic Hg enrichment is important because it directly affects future environmental

responses to changes in anthropogenic emissions, and we discuss the implications of various uncertainty scenarios here. We re-examine evidence for anthropogenic enrichment of atmospheric deposition in published peat records and compare results to recent reviews of lake sediment data. We use a global geochemical model for Hg cycling to explore impacts of historical Hg emissions scenarios on global anthropogenic enrichment and evaluate consistency of modeling scenarios with archival data and contemporary measurements. Implications of various historical Hg emissions scenarios for future environmental concentrations and responses to emissions reductions are presented.

2.0. METHODS

2.1. Model Description. We use the global biogeochemical box model developed by Amos et al.²¹ and updated to include burial in coastal sediments³ to investigate the environmental implications of major uncertainties in Hg emissions and cycling. The model represents Hg cycling as a set of coupled ordinary differential equations based on first-order rate coefficients (k) for Hg exchange between seven global reservoirs, as described in previous work. Model reservoirs represent three types of terrestrial Hg pools, three ocean compartments, and the atmosphere. The model is initialized from a natural steady-state simulation without anthropogenic Hg releases and then forced from 2000 BC to present day (2008 AD) with anthropogenic Hg releases. The size of modeled present-day Hg reservoirs and the magnitude of anthropogenic enrichment are compared to observations. All parameter values are provided in the Supporting Information of Amos et al.,³ and the model is publicly available at <http://bgc.seas.harvard.edu/models.html>.

Table 1 describes six sensitivity simulations that explore uncertainty in historical atmospheric Hg emissions and model rate coefficients that describe how Hg cycles through the environment. Sensitivity simulations include scenarios: (1 and 2) reduced anthropogenic emissions from pre-1900s mining, (3) increased geogenic emissions, (4) elevated oceanic evasion, (5) reduced terrestrial re-emissions, and (6) greater burial at ocean margins. We evaluate the plausibility of each model scenario using observational constraints on the following: (a) anthropogenic enrichment factors from archival records, (b) the timing of peak Hg inputs, and (c) the size of present-day global Hg reservoirs derived from contemporary measurements of Hg concentrations in the atmosphere, ocean, and soils.

2.2. Constraints on Anthropogenic Enrichment from Natural Archives. We compile available data from remote ombrotrophic peat bogs (Supporting Information (SI) Table S1) to investigate changes in historical atmospheric Hg deposition and anthropogenic enrichment across archives from different regions. This includes the compilation of peat

data from Biester et al.¹⁵ and other recent studies. Varved or ¹⁴C dated lake sediment records covering the centuries before Hg use in large-scale mining (i.e., pre-16th century) are included as well (SI Table S1). Shorter sediment records (~150 years) have been recently reviewed elsewhere.^{13,32} We do not conduct an additional review of ²¹⁰Pb dated cores, except to discuss the Biester compilation of sediment data as it relates to previous interpretation of peat.

We calculate a series of enrichment factors (EFs), defined as the ratio of Hg accumulation rates ($\mu\text{g m}^{-2} \text{ year}^{-1}$) from two time intervals. EFs are calculated for four periods based on two historical reference periods: (a) “pre-industrial” (1760 to 1880) and (b) before the rise of large-scale gold, silver, and Hg mining (3000 BC to 1550 AD).³³ Longer, varved or ¹⁴C dated lacustrine sediment records and multimillennial ¹⁴C dated peat records are used to derive EFs relative to 3000 BC to 1550 AD. Relative accumulation is calculated for two modern periods: (a) contemporary (ca. post-1990) Hg accumulation and (b) the extended 20th century maximum (“20Cmax”) observed in most archival records (SI Tables S1). These intervals are determined empirically based on the temporal resolution of the archives. We average Hg accumulation rates across the most pronounced 20th century peak, which is typically between the 1940s and 1980s. Supporting Information Table S1 documents the onset and end of the 20Cmax in peat and sediment archives. The Hg accumulation rates and EFs for each core are documented in SI Table S1, as well as the onset and end of the 20Cmax. We perform the Shapiro–Wilk test for normality. We average EFs for studies with multiple cores per site. If data are normally distributed, we report mean \pm standard deviation (SD). If data are not normally distributed, we report the median and 95% confidence intervals.

2.3. Constraints on Present-Day Global Hg Reservoirs.

Direct measurements of contemporary Hg concentrations in the atmosphere, ocean, and soils can be used to constrain modeled sizes of Hg reservoirs. Recent models evaluated against direct measurements of atmospheric Hg estimate that the atmosphere contains approximately 5000 Mg of Hg (range, 4600–5600 Mg; reviewed in Amos et al.²¹). Atmospheric Hg is measured with a time resolution of minutes to hours at more than 30 land-based stations.^{34,35} Other data include measurements from ship cruises^{36–39} and aircraft measurements spanning the globe,^{40–44} as well as numerous field studies (e.g., see Rutter et al.⁴⁵ and Jaffe et al.⁴⁶). Given the abundance of atmospheric Hg measurements, the size of the present-day atmospheric reservoir is one of the strongest constraints on the global Hg budget.

Mean seawater Hg concentrations range between 0.6 and 2.9 pM in the upper 1000 m of the ocean and between 0.5 and 2.4 pM below 1000 m and can be used to constrain the contemporary oceanic Hg reservoir.^{29,47,48} Sunderland and Mason¹⁷ compiled all available seawater Hg measurements prior to 2005 and estimated the Hg reservoir in the global ocean at 350 Gg (90% confidence interval, 270–450 Gg), of which approximately 18% (63–120 Mg) is above 1000 m. Lamborg et al.²⁹ synthesized more recent observations, mainly from GEOTRACES cruises post-2005, and estimated the total oceanic reservoir at 280 Gg. This is similar to the recent modeling results (260 Gg) by Zhang et al.³² The upper ocean reservoir estimate from Lamborg et al.²⁹ falls on the low end of the earlier estimates of Sunderland and Mason¹⁷ at 63 Mg, indicating a general pattern of lower Hg concentrations measured in recent cruises. This could be either a temporal

trend or a result of contamination of earlier samples and remains an open question.⁴⁸

The size of the global soil Hg reservoir is less certain due to sparser observational coverage and large variability across ecosystems and soil profiles. There have been two independent model estimates of global Hg storage in soils. Smith-Downey et al.⁴⁹ developed a mechanistic model for terrestrial Hg cycling based on soil organic carbon dynamics that builds on their strong association^{50–55} and evaluated the model against two continental scale transects across the United States and Canada.⁵⁶ This study estimated the terrestrial Hg reservoir to be ~240 Gg globally. Hararuk et al.⁵⁷ estimated a reservoir of approximately 15 Gg in the upper 40 cm of U.S. soils using more recent field measurements. Extrapolating measured organic carbon-to-Hg ratios globally results in more than 300 Gg suggesting results from Smith-Downey et al.⁴⁹ may have underestimated Hg contained in the terrestrial environment. A number of additional studies from a diversity of geographic locations have reported soil Hg concentrations from upland soils (SI Table S2). Mean Hg concentrations in North American and European soils distant from point sources generally fall between 20 and 50 ng g⁻¹ dry weight (SI Table S2), which is in the range of the two studies previously used to estimate magnitudes of global reservoirs. Recently reported soil concentrations from east Asia are higher on average (SI Table S2), implying even 300 Gg may be biased low.

2.4. Primary Anthropogenic Emissions. Enrichment of anthropogenic Hg in environmental reservoirs is determined by the magnitude of historical anthropogenic releases and the time scales of coupling among reservoirs that affect reemissions and sequestration. Uncertainty in historical anthropogenic emissions plays a large role in modeled enrichment of environmental reservoirs. Horowitz et al.²⁰ estimated that globally 320 Gg of Hg has been cumulatively released to the atmosphere since 1850 by including environmental releases associated with intentional uses of Hg in commercial products and processes (Figure 1; Table 2). The earlier inventory developed by Streets et al.¹⁹ estimated 130 Gg (80% CI, 70–260 Gg) was released prior to 1850, primarily associated with silver mining in colonial Spanish America between the 16th and 19th centuries. The model from Amos et al.³ is forced by the inventory from Horowitz et al.,²⁰ which suggests global emissions to the atmosphere peaked in the 1970s at the height of Hg use in products such as batteries and paint.

We investigate the environmental implications of uncertainty in historical Hg emissions from large-scale mining prior to the 20th century by considering alternate emissions scenarios proposed in recent work. Over the past several centuries, mining has been the dominant anthropogenic source of Hg to the environment and the principal driver of early enrichment. Historical mining emissions are uncertain, especially with regard to the proportion of Hg used in mining that was lost to the atmosphere as Hg(0). Scenario 1 decreases pre-1920 mining emissions from Streets et al.¹⁹ by a factor of 3 as suggested by Zhang et al.³² (SI Figure S1). Scenario 2 reduces 1850-to-1920 mining emissions by 50% and eliminates pre-1850 emissions (SI Figure S1). Large-scale mining contributes a relatively small portion to global anthropogenic emissions after the 1920s when Hg amalgamation was largely replaced by cyanide extraction.⁵⁸

2.5. Sources of Geogenic Emissions. The magnitude of geogenic emissions establishes natural levels of Hg in the atmosphere. Geogenic emissions were 90 Mg year⁻¹ in Amos et

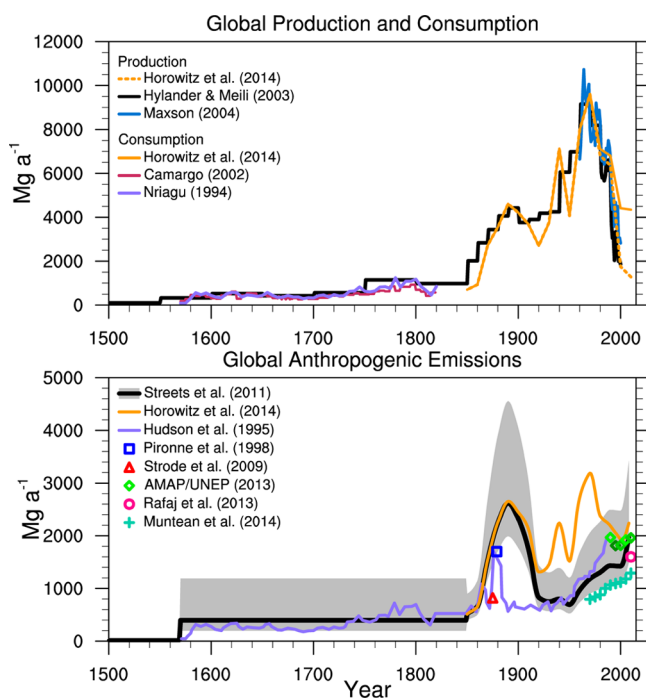


Figure 1. Published estimates of global Hg production and consumption (top panel) and primary anthropogenic emissions of Hg to the atmosphere (bottom panel).^{19,20,22–25,27,28,121–123,125}

al.³ based on passively degassing volcanoes⁵⁹ and are updated to $76 \pm 30 \text{ Mg year}^{-1}$ here based on the most recent work from

the same group.⁶⁰ We investigate the biogeochemical implications of the upper end of uncertainty in total geogenic emissions (300 Mg year^{-1})²¹ as our third uncertainty scenario. The contribution from large eruptions (2000–5000 Mg of Hg per event, 1–2 times per century⁶¹) is small when integrated over time. Cumulative release from large eruptions since 1850 comprise <5% of total anthropogenic emissions over the same time period, which is similar to the fraction estimated by Schuster et al.⁶² using ice core data. Hydrothermal vents are a small source to marine waters^{48,63} and are not considered here. The upper range estimate for total geogenic emissions thus depends on substantial emissions from naturally enriched soils, which is constrained based only on data from Nevada, USA.⁶⁴

2.6. Variability in Oceanic Evasion Rates. The magnitude of air–sea exchange has a major influence on the reservoir of Hg retained in the ocean and available for conversion to bioaccumulative MeHg.³⁶ Concentrations of dissolved Hg(0) in seawater are driven by (1) the supply of inorganic Hg(II), (2) biological and photochemical reaction rates mediated by light availability and bacterial activity, and (3) the stability of Hg(II) complexes in seawater.⁶⁵ Air–sea exchange measurements from multiple marine waters and inland seas^{36,66–72} suggest net fluxes range from 0.4 to 4.2 ng m⁻² h⁻¹ (SI Table S3). Environmental drivers of variability in photochemical and biological Hg redox reactions have only been measured in a few studies.^{73–77} Modeled net global evasion based on this work is approximately $3000 \text{ Mg year}^{-1}$ (90% confidence interval,¹⁷ 2000–4000 Mg year⁻¹), which results in a spatial and annual average of $0.9 \text{ ng m}^{-2} \text{ h}^{-1}$.⁶⁵ Using observational constraints, Amos et al.²¹ estimated

Table 2. Literature Estimates of Primary Hg Sources to the Environment^a

source	annual release (Mg year ⁻¹)	cumulative release (Gg)
Geogenic		
emissions to the atmosphere		
volcanoes, passive degassing	76 ± 30^b $\sim 100^d$	12 ± 5^c $\sim 16^c$
volcanoes, large sporadic eruptions	2000–5000 Mg per event ^e	$>4^f$
geothermal	60 ^g	9.6 ^c
releases to water		
sea floor hydrothermal vents	$<20^h$	$<3.2^c$
Anthropogenic		
emissions to the atmosphere		
2005	1900 ⁱ , 2000 ^j	
2008	2000 (1300–3200) ^k , 1300 ^l	
2010	2000 (1000–4100) ^m , 1600 ⁿ , 2400 ^o	
since 1850		220 (140–370) ^{k,p} , 320 ^o
all time		350 (230–790) ^{k,p}
releases to land and water		
2010	1100 (550–1900) ^{m,q} , 1400 ^{o,r}	
since 1850		310 ^{o,s}

^aPyle and Mather⁶¹ estimate small sporadic volcanic eruptions release 500 (60–2000) Mg of Hg year⁻¹. Emissions from geologically enriched soils along the world's mercuriferous belts have been estimated to be between 500 and 750 Mg year⁻¹.⁶⁴ The analysis here suggests these may be overestimated based on empirical constraints on the global Hg cycle (see Figure 4 and text in Section 3.0). ^bBagnato et al.⁶⁰ Assuming a constant emission rate between 1850 and 2010. ^dBagnato et al.;⁵⁹ Mather et al.;¹¹⁷ Andren and Nriagu.² ^ePyle and Mather.⁶¹ ^fFor four large eruptions between 1850 and 2010. Large eruptions occur at a frequency of 1–2 times per century. ^gVarekamp and Buseck.¹¹⁸ ^hLamborg et al.⁶³ for total dissolved Hg (and MMHg) inputs. ⁱWilson et al.¹¹⁹ ^jPacyna et al.¹²⁰ ^kStreets et al.¹⁹ ^lMuntean et al.¹²¹ ^mAMAP/UNEP.¹²² ⁿRafaj et al.¹²³ ^oHorowitz et al.²⁰ Note this inventory includes commercial products missing from previous emission estimates. ^pRange represents 80% confidence intervals. ^qIncludes primary anthropogenic releases of 190 (range, 40–580) Mg year⁻¹ to water, plus ASGM releases to land and water of 880 (range, 500–1300) Mg year⁻¹. ^rReleases to water are 560 Mg year⁻¹, and releases to land are 790 Mg year⁻¹. ^sCumulative releases to water are 160 Gg, and releases to land are 150 Gg.

uncertainty in the first-order rate coefficient for Hg(0) evasion from the surface ocean is $\pm 30\%$ and we explore this as the fourth uncertainty scenario.

2.7. Variability in Atmospheric–Terrestrial Exchange of Hg(0). A substantial proportion of the atmospherically deposited Hg(II) to soils, on leaf surfaces and vegetation, ice, and snow is photochemically, abiotically, and/or biologically reduced and evaded back to the atmosphere as Hg(0).^{78–82} For example, Graydon et al.⁸³ found that 45–70% of isotopically labeled Hg(II) wet deposited to a forested watershed had been re-emitted to the atmosphere after 1 year. No study has experimentally assessed the re-emission potential for other forms of deposition such as stomatal uptake and re-release of Hg(0) or the fate of particulate-bound Hg. Using a global model, Smith-Downey et al.⁴⁹ estimated 56% of annual atmospheric deposition is re-emitted. Recent observations suggest less evasion of Hg(0) from soils and therefore higher storage than previously thought.⁸⁴ This implies smaller first-order rate coefficients for Hg(0) evasion from soils to the atmosphere globally, which we explore as a fifth model scenario.

2.9. Sequestration of Hg in Marine Sediments. Sediment burial at ocean margins is the largest sink of anthropogenic Hg globally.³ Present-day global mean Hg discharges from rivers based on Hg concentrations measured at or near river mouths range from 1000 to 5500 Mg year⁻¹.^{3,17,85} Settling and burial of 70–90% of the suspended particle load in rivers prior to reaching the open ocean^{3,86} is equivalent to a deposition flux of 20–130 $\mu\text{g m}^{-2} \text{ year}^{-1}$, within the range of observed Hg settling fluxes in estuaries and on the shelf (60–700 $\mu\text{g m}^{-2} \text{ year}^{-1}$).^{85,87–95} The upper estimate of global Hg discharge (5500 Mg year⁻¹)³ reflects the inclusion of recent measurements from large, highly contaminated Asian rivers. Burial in deep ocean sediments is estimated to be 190 Mg year⁻¹ (90% confidence interval, 180–260 Mg year⁻¹)¹⁷ and is a comparatively less important sink. As the sixth uncertainty scenario, we increase the percent of permanent burial at ocean margins from 70% to 90% to accommodate previously published ranges. Disturbance of buried estuarine and shelf sediments through benthic trawling, dredging, and coastline development has been widespread in recent decades and may effectively lower this sequestration term. However, the temporal and spatial extent of these effects has not been quantified and thus cannot be considered here.

3.0. RESULTS AND DISCUSSION

3.1. Pre-industrial-to-Present Enrichment. Supporting Information Table S1 summarizes relative changes in Hg accumulation rates in peat records for the four time periods considered in this analysis. We refer to the period of maximal Hg accumulation as the extended 20th century maximum (abbreviated 20Cmax). Median 20Cmax occurs in 1960 (95% confidence interval, 1940 to 1977; $n = 20$) in peat records and 1960 (95% CI, 1953 to 1982; $n = 70$) in lake sediments (SI Table S1).

Our analysis of peat records suggests the choice of pre-industrial reference period explains most of the previously reported discrepancy between lake sediment and peat. Biester et al.¹⁵ reported median pre-industrial-to-present enrichment of 3 ± 1 for lake sediments and 40 for peat. The authors used 1760 to 1880 as a reference period for sediment and 3000 BC to 1550 AD as a reference for peat, leading to more than a factor of 10 difference in reported EFs. Correcting the reference period for peat to 1760 to 1880, we calculate a median

enrichment factor of 4.6 (2.3–14; $n = 19$) with all data included and 4.3 if the Shotyk et al.⁹⁶ outlier is excluded (2SD outlier test; see SI Table S1). There is still a statistically significant difference ($p < 0.001$) in enrichment between sediment and peat. Differences between sediment and peat enrichment may be explained by the delayed release of Hg from catchment soils and longer time scales of accumulation associated with watershed dynamics^{10,97,98} or by potential ²¹⁰Pb dating issues with both peat¹⁵ and sediment cores.^{99,100} It has been argued ²¹⁰Pb is mobile in the surface layers in some bogs, introducing bias in age dating and overestimation of recent Hg accumulation rates.¹⁵ Establishing a reliable ²¹⁰Pb chronology in any archive requires validation by an independent time marker (e.g., ¹⁴C, ¹³⁷Cs, ^{239,240}Pu, varves, known episodic events)^{101–103} but is lacking for many sediment records.

Figure 2 illustrates how the signal of atmospheric Hg deposition can be dampened by longer time scales of accumulation. Figure 2 shows modeled atmospheric deposition, the fast terrestrial reservoir and slow terrestrial reservoir for several model scenarios (Table 1) to characterize a range of possible histories of Hg accumulation. The signal of enrichment diminishes as the temporal integration of inputs increases from

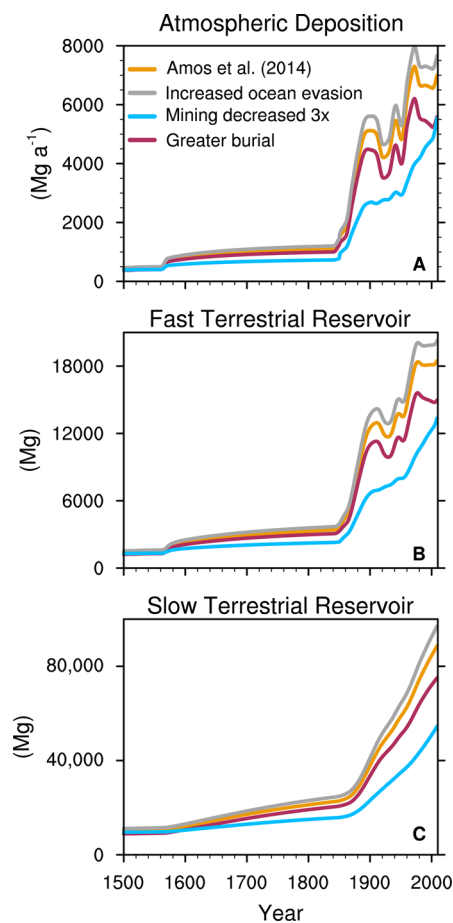


Figure 2. Modeled effects of variable time scales of integration on the signal of atmospheric Hg deposition recorded in terrestrial ecosystems. Atmospheric deposition (panel A) is based on the model scenarios described in Table 1. Panel B shows the response of the fast terrestrial reservoir with a lifetime of less than a decade, which is analogous to the temporal resolution of peat archives. The slow terrestrial reservoir shown in panel C has a lifetime of decades or more and is analogous to the time scales of accumulation for most lake sediment records.

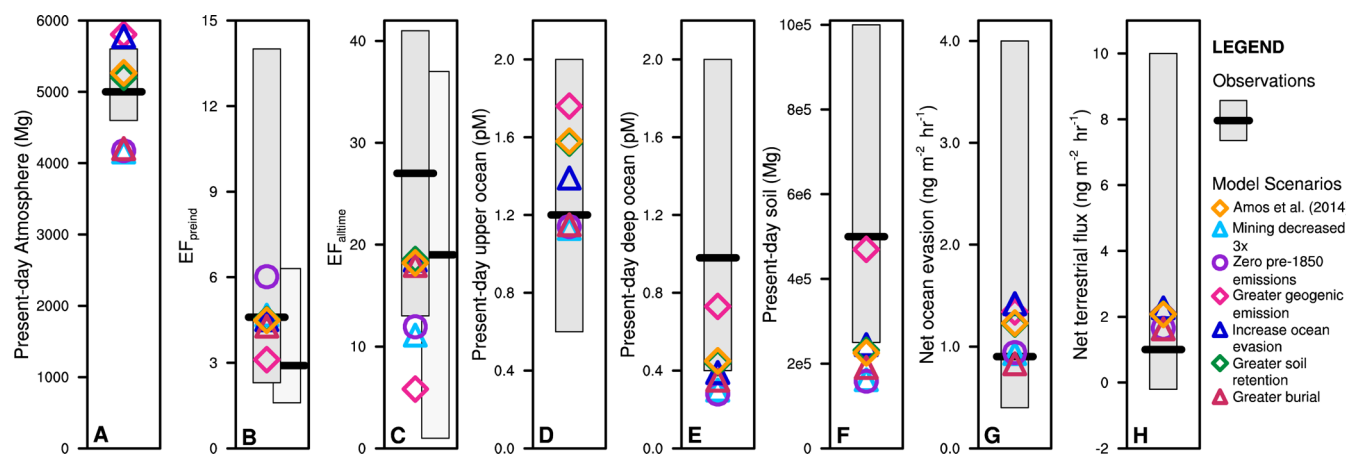


Figure 3. Observational constraints (gray bars) on model sensitivity simulations (symbols). Thick black horizontal lines indicate the observational mean or best estimate and median $\pm 95\%$ confidence intervals for panel B (see text). For panels B and C, EFs from peat are shown as the darker gray bar and lighter gray bar for lake sediments. Table 1 describes each model scenario. For archives, EF_{preind} = the ratio of mean Hg accumulation rate from the extended 20th century maximum (“20Cmax”) relative to pre-industrial (1760 to 1880) and $EF_{alltime}$ is the ratio 20Cmax relative to pre-large-scale mining (3000 BC to 1550 AD). Model EFs are calculated from atmospheric deposition, and 20Cmax is taken as 1950 to 1975 based on peak emissions in Horowitz et al.²⁰ (Figure 1).

Table 3. Emission Factors Associated with Mercury, Silver^a, and Gold^a mining

type of mining ^b	region	time period	% emitted to the atmosphere	ref
Hg, large scale	Huancavelica, Peru	colonial	25	Robins and Hagan ²⁶
Ag, large scale	Potosi, Bolivia	colonial	85 ^c	Robins ¹⁰⁵
Ag, large scale		colonial	7–34 ^d	Guerrero ¹⁰⁶
Ag and Au, large scale	Americas	colonial–gold rush	60–65	Nriagu ^{28,108}
Ag and Au, large scale	global	1850–1880	40 ^e	Streets et al. ¹⁹
Ag and Au, large scale	global	post-1880	15–39 ^f	Streets et al. ¹⁹
Au, artisanal	Amazon	modern	65–87 ^e	Lacerda ¹⁰⁴
Au, artisanal	global	modern	45 ^e	AMAP/UNEP ¹²²
Hg, artisanal	Guizhou, China	modern	7–32	Li et al. ¹²⁴

^aFor Hg amalgamation methods only. ^bHg = mercury, Ag = silver, and Au = gold. ^cLost to the atmosphere in the initial or one of the subsequent firings. ^dAssumes 100% recovery of Hg during firing and washing without losses to the environment but does not include reprocessing of recovered Hg. ^eAssumes no recovery of Hg. ^fIncludes some recovery of Hg.

years (fast terrestrial reservoir) to decades (slow terrestrial reservoir). In Amos et al.³ (Figure 2, orange line), the enrichment from 1760 to 1880 to 20Cmax is a factor of 4.4 for atmospheric deposition, 4.0 for the fast terrestrial reservoir, and 2.9 for the slow terrestrial reservoir. This pattern supports the premise that differences in median peat and sediment enrichment may in large part reflect differences in time scales of Hg accumulation and associated coupling with the atmospheric deposition signal.

3.2. Evidence for Pre-1850 Anthropogenic Impacts. In peat records, pre-industrial (1760 to 1880) Hg accumulation rates are a factor of 5 greater than pre-mining accumulation (3000 BC to 1550 AD). The mean increase in Hg accumulation from the pre-mining era to the 20Cmax in peat is a factor of 27 (SD, ± 14 ; median = 26; $n = 14$). Mean enrichment from varved or ¹⁴C lake sediment is a factor of 17 (SD, ± 17 ; median = 14; $n = 7$). Mean sediment and peat enrichment factors are not significantly different (t test, $p = 0.21$), but there is substantial variability in the precolonial Hg accumulation in the seven lake sediment records. Modeled enrichment in atmospheric deposition from Amos et al.³ over the same period is 18 and ranges from 6 to 19 across uncertainty scenarios (Figure 3C). Multiple lines of evidence for enrichment in atmospheric Hg deposition before the pre-industrial

(1760 to 1880) era from sediment, peat, and modeling all support early anthropogenic enrichment of the global Hg cycle.

The historical pattern of Hg consumption is well documented (Figure 1). Associated emissions to the atmosphere are more uncertain, as illustrated by the range of proposed historical emission profiles (Figures 1 and S1 (Supporting Information)). Hg consumed for large-scale silver mining in colonial South America grew rapidly following the discovery of the *patio* amalgamation process in the 1550s.¹⁰⁴ Mercury use for amalgamation in large-scale mining peaked in the late 1800s^{23,28} at approximately 4600 Mg of Hg year⁻¹²⁴ which is comparable to contemporary global consumption.⁵⁸

Variability in the emission factor for historical silver mining and uncertainty about calomel (Hg₂Cl₂(s)) formation during the processing of silver ores are the major contributors to uncertainty in pre-1900s atmospheric emissions. The amalgamation process began by crushing silver ore, combining it with water, Hg, salt, and other ingredients, and spreading it out on a patio. Humans tread on the mixture to accelerate amalgamation. The paste was rinsed and runoff was recaptured and reused. Once separated, the amalgam was squeezed through cloth to further remove excess Hg. The amalgam was fired in kilns, leaving behind pure silver and releasing Hg(0) vapor. More detail on the amalgamation process can be found elsewhere.^{26,105}

Estimated atmospheric releases range from 7 to 85% of total Hg consumed (Table 3).^{26,105–108} The low end of this range (7–34%) favors extensive calomel formation and assumes 100% recovery of Hg during washing without losses to the environment.¹⁰⁶ This is unlikely given the porous ceramic materials used in smelting that would release substantial quantities of Hg as vapor^{105,107,109} and ignores the extensive reprocessing of refining byproducts enriched in silver and Hg, as well as the use of Hg captured in the smelting process. Substantial quantities of Hg are known to leach from wasted calcines (roasted ores).^{110–112} Leaching and subsequent volatilization from mine wastes are currently not accounted for in loss estimates.

3.3. Changes in the Modern Era. Archival observations and geochemical modeling both provide evidence for peak atmospheric Hg concentrations during the second half of the 20th century and declines in more recent decades. Peat records indicate Hg accumulation has declined by a factor of 2.2 (median; 1.5–9.0; $n = 14$) from the 20C max to the modern era (post-1990s). Most lake sediments show a more gradual decrease, or no decrease, in Hg accumulation since the 20Cmax (factor, 0.9; 95% CI, 0.7–1.5; $n = 70$), which was also found independently by Zhang et al.³² ($n > 100$ cores). As shown in Figure 2, greater temporal integration of Hg accumulated through both watershed influences and in-lake processes can explain time averaged or slow changes in sediment Hg accumulation rates in response to changes in atmospheric Hg emissions.

Variability in Hg concentrations over the past several decades recorded in an ice core,⁶² firn air,⁶ and snow from central Greenland¹¹³ corroborate the occurrence of a 20Cmax between the 1940s and 1980s and a subsequent decline. Greenland snow cores at Summit revealed Hg concentrations that were 1.7-fold higher in 1948–1965 than in 1965–1988.¹¹³ Interstitial air in firn from Summit, Greenland shows a 2-fold increase in Hg(0) from 1940 to 1970, followed by a 1.8-fold decrease to modern levels.⁶ This 20th century peak in anthropogenic emissions is also accounted for in the global inventory from Horowitz et al.²⁰

3.4. Uncertainty in Anthropogenic Hg Emissions and Biogeochemical Cycling. Here we present six sensitivity simulations that explore the impact of uncertainty in Hg cycling and atmospheric emissions on anthropogenic enrichment. The plausibility of each scenario is assessed against multiple independent lines of observation. Figure 3 shows the model outcomes from the six uncertainty scenarios (Table 1) evaluated against the observational constraints described in section 2.0. Historical emissions scenarios that decrease releases from mining by a factor of 3 or exclude pre-1850 anthropogenic emissions (SI Figure S1) fall below the observational constraints for the atmosphere, terrestrial ecosystems, and deep ocean (Figure 3A,E,F). All-time enrichment in atmospheric deposition from these low historical emissions scenarios also fall outside the 95% confidence intervals of observed peat enrichment factors (“EF_{alltime}” in Figure 3C) and are biased low relative to the mean enrichment from lake sediments. A proposed rationale for decreasing global emissions from early mining by 50–66% (scenarios 1 and 2, SI Figure S1) is that most Hg used for amalgamation ended up as calomel instead of being volatilized to the atmosphere.¹⁰⁶ The comparison in Figure 3 demonstrates that making this assumption worsens agreement with multiple independent measurements and by

extension suggests the fraction of Hg emitted must have been large and the impact global.

Figure 3A shows that increasing geogenic emissions to the atmosphere to their upper limit (300 Mg year⁻¹) in the model biases the present-day atmosphere outside the observational range. High geogenic emissions bias the upper ocean concentrations high with respect to mean concentrations (Figure 3D). Field observations suggest that global Hg emissions from volcanoes are 76 ± 30 Mg year⁻¹,⁶⁰ suggesting the additional contribution from Hg enriched soils is 200 Mg year⁻¹ or less.

Recent research on Hg contained in terrestrial ecosystems^{57,114} suggests greater Hg retention in soils on a global scale than previously realized (scenario 5, Table 1). Figure 3 shows that decreased Hg emissions from soils are consistent with the range of available observational constraints. Increasing Hg retention in soils also implies a reduction in oceanic Hg accumulation, which is consistent with lower Hg concentrations in seawater from recent measurements (see section 2.3). The scenario for increased oceanic evasion lowers modeled surface ocean concentrations but results in an atmospheric reservoir and deep ocean that fall outside observational constraints. Similarly, increasing burial of Hg in ocean margins lowers modeled seawater Hg concentrations in the upper ocean (Figure 3D) but results in a large low bias with respect to the atmosphere, deep ocean, and soil reservoirs (Figure 3A,E,F).

3.5. Implications for Future Responses. Figure 4 shows relative changes in atmospheric and oceanic Hg concentration following the elimination of all primary anthropogenic Hg emissions to the atmosphere in 2015 for several model uncertainty scenarios. Although eliminating emissions in hypothetical, it allows us to directly compare environmental responses across sensitivity simulations. Results show relatively little difference among base-case model scenario and lower Hg emissions from mining, increased Hg removal through burial, and high air–sea exchange on future responses. The atmosphere responds immediately under all emissions scenarios to the termination of future emissions, which is consistent with contemporary measurements showing rapid decreases in atmospheric deposition in response to decreasing emissions.^{115,116} This reflects the relatively short lifetime of Hg against removal (0.5–1 year). Removing the full anthropogenic perturbation to the global biogeochemical requires longer time scales as reflected by the growth of the Hg reservoir in the deep ocean over the 21st century. The amount of Hg sequestered in ocean margin sediments (burial) has the greatest impact on future concentration trends across all geochemical reservoirs (Figure 4).

Figure 4 also illustrates how the profile (i.e., shape) of past emissions impacts future trajectories. Amos et al.³ (Figure 4, orange line) is forced by the Horowitz et al.²⁰ emission inventory, where there is a rapid drop in global anthropogenic emissions after the 1970s and emissions only begin to increase after 2000 (Figure 1) due to growth in Asia. Conversely, the scenario labeled “mining decreased 3×” (cyan line) is based on Streets et al.,¹⁹ which does not include commercial products, and global emissions have monotonically increased since the 1970s. Even though upper ocean concentrations start lower in 2016 under the decreased mining emission scenario, the recovery after terminating emissions is notably slower because global emissions steadily climbed from the 1970s to present. The implication is that the near-term response of upper ocean concentrations to future regulations is particularly sensitive to

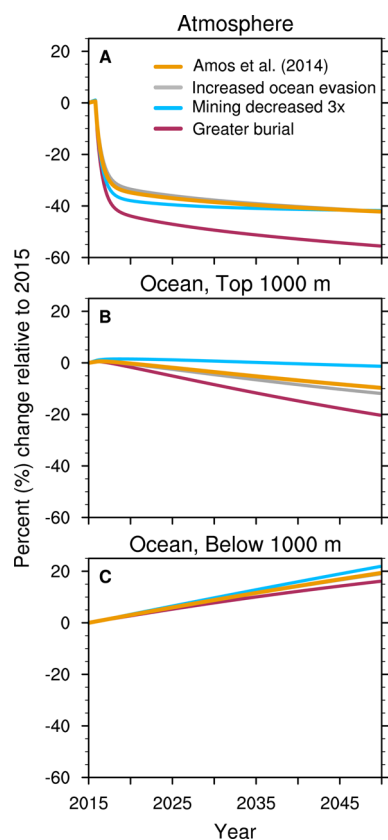


Figure 4. Modeled relative changes in Hg concentrations in the atmosphere and ocean following termination of all primary anthropogenic emissions in 2016. Results are normalized to 2015 and expressed as percent (%) change in concentrations. Relative responses of the atmosphere (A), upper ocean (B), and deep ocean (C) are shown for the base-case simulation developed by Amos et al.³ and scenarios that increase oceanic mercury evasion by 30%, decrease mining emissions by a factor of 3, and increase sequestration of Hg in ocean margin sediments from 70% to 90% as described in Table 1.

the profile (i.e., shape) of anthropogenic emissions in recent decades.

Rapid declines in atmospheric and surface ocean concentrations in response to changes in anthropogenic Hg emissions to the atmosphere are robust to the uncertainties considered in this analysis. Aggressive reduction of global Hg emissions is needed to stabilize subsurface and deep oceanic Hg levels irrespective of the uncertainty in historical emissions and biogeochemical cycling considered.

Using a combination of measurements and modeling, this analysis shows early mining emissions have had a substantial impact on global all-time anthropogenic enrichment. Mercury accumulation rates in peat increased by a factor of 4.3 (median) from pre-industrial (1760–1880) to the 20Cmax, compared to a factor of 3.0 (median) for lake sediment. Median Hg accumulation rates in both peat and sediment are a factor of ~5 lower during the precolonial period (3000 BC to 1550 AD) than during the pre-industrial period (1760 to 1880), which is in agreement with model simulations that have also been constrained by contemporary measurements. Important research directions for better anticipating the impacts of legacy anthropogenic Hg in coming decades include improved quantification of the retention of atmospherically deposited Hg in soils, disturbance of Hg buried in coastal sediment, and air–sea exchange.

■ ASSOCIATED CONTENT

📄 Supporting Information

Tables listing a summary of Hg accumulation rates for each lake sediment and peat record used in this analysis and empirical ranges of Hg concentrations in soils, terrestrial Hg(0) evasion, and ocean Hg(0) evasion, figure showing plot of alternate historical emission scenarios, and text giving accompanying references. This material is available free of charge via the Internet at <http://pubs.acs.org>.

■ AUTHOR INFORMATION

Corresponding Author

*Phone: +1 (617) 496-5348; fax: +1 (617) 495-4551; e-mail: hamos@hsph.harvard.edu.

Notes

The authors declare no competing financial interest.

■ ACKNOWLEDGMENTS

We thank the Editor and anonymous reviewers for their thoughtful comments. This manuscript was initiated by the special session entitled “Defining Natural and Anthropogenic Mercury” convened at the 11th International Conference on Mercury as a Global Pollutant in Edinburgh, Scotland in July, 2013. Financial support for work at Harvard was from the U.S. Environmental Protection Agency Contract No. EP-11-H-0013646. J.E.S. acknowledges funding from the European Research Council (Grant ERC-2010-StG_20091028). H.M.A. acknowledges use of NCL software version 6.1.2 (<http://www.ncl.ucar.edu/>) to create Figures 1–4 and the table of contents/abstract artwork.

■ REFERENCES

- (1) Mason, R. P.; Fitzgerald, W. F.; Morel, F. M. M. The biogeochemical cycling of element mercury—Anthropogenic influences. *Geochim. Cosmochim. Acta* **1994**, *58* (15), 3191–3198.
- (2) Andren, M. O.; Nriagu, J. O. *The global cycle of mercury*; Elsevier: Amsterdam, 1979.
- (3) Amos, H. M.; Jacob, D. J.; Kocman, D.; Horowitz, H. M.; Zhang, Y.; Dutkiewicz, S.; Horvat, M.; Corbitt, E. S.; Krabbenhoft, D. P.; Sunderland, E. M. Global biogeochemical implications of mercury discharges from rivers and sediment burial. *Environ. Sci. Technol.* **2014**, *48* (16), 9514–9522.
- (4) Dietz, R.; Outridge, P. M.; Hobson, K. A. Anthropogenic contributions to mercury levels in present-day Arctic animals—A review. *Sci. Total Environ.* **2009**, *407* (24), 6120–6131.
- (5) Swain, E. B.; Engstrom, D. R.; Brigham, M. E.; Henning, T. A.; Brezonik, P. L. Increasing rates of atmospheric mercury deposition in midcontinental North America. *Science* **1992**, *257* (5071), 784–787.
- (6) Fain, X.; Ferrari, C. P.; Dommergue, A.; Albert, M. R.; Battle, M.; Severinghaus, J.; Arnaud, L.; Barnola, J. M.; Cairns, W.; Barbante, C.; Boutron, C. Polar firm air reveals large-scale impact of anthropogenic mercury emissions during the 1970s. *Proc. Natl. Acad. Sci. U. S. A.* **2009**, *106* (38), 16114–16119.
- (7) Givélet, N.; Roos-Barraclough, F.; Shoty, W. Predominant anthropogenic sources and rates of atmospheric mercury accumulation in southern Ontario recorded by peat cores from three bogs: Comparison with natural “background” values (past 8000 years). *J. Environ. Monit.* **2003**, *5* (6), 935–949.
- (8) Vandal, G. M.; Fitzgerald, W. F.; Boutron, C. F.; Candelone, J. P. *Mercury in ancient ice and recent snow from the Antarctic*. Springer-Verlag: Berlin, 1995; Vol. 30, p 401–415.
- (9) Goodsite, M. E.; Outridge, P. M.; Christensen, J. H.; Dastoor, A.; Muir, D.; Travnikov, O.; Wilson, S. How well do environmental archives of atmospheric mercury deposition in the Arctic reproduce

rates and trends depicted by atmospheric models and measurements? *Sci. Total Environ.* **2013**, *452*, 196–207.

(10) Outridge, P. M.; Rausch, N.; Percival, J. B.; Shoty, W.; McNeely, R. Comparison of mercury and zinc profiles in peat and lake sediment archives with historical changes in emissions from the Flin Flon metal smelter, Manitoba, Canada. *Sci. Total Environ.* **2011**, *409* (3), 548–563.

(11) Sunderland, E. M.; Cohen, M. D.; Selin, N. E.; Chmura, G. L. Reconciling models and measurements to assess trends in atmospheric mercury deposition. *Environ. Pollut.* **2008**, *156* (2), 526–535.

(12) Lindberg, S.; Bullock, R.; Ebinghaus, R.; Engstrom, D.; Feng, X.; Fitzgerald, W.; Pirrone, N.; Prestbo, E.; Seigneur, C. A synthesis of progress and uncertainties in attributing the sources of mercury deposition. *Ambio* **2007**, *36*, 19–32.

(13) Engstrom, D. R.; Fitzgerald, W. F.; Cooke, C. A.; Lamborg, C. H.; Drevnick, P. E.; Swain, E. B.; Balogh, S. J.; Balcom, P. H. Atmospheric Hg emissions from preindustrial gold and silver extraction in the Americas: A reevaluation from lake-sediment archives. *Environ. Sci. Technol.* **2014**, *48* (12), 6533–6543.

(14) Drevnick, P. E.; Yang, H. D.; Lamborg, C. H.; Rose, N. L. Net atmospheric mercury deposition to Svalbard: Estimates from lacustrine sediments. *Atmos. Environ.* **2012**, *59*, 509–513.

(15) Biester, H.; Bindler, R.; Martinez-Cortizas, A.; Engstrom, D. R. Modeling the past atmospheric deposition of mercury using natural archives. *Environ. Sci. Technol.* **2007**, *41* (14), 4851–4860.

(16) Mason, R. P.; Sheu, G. R. Role of the ocean in the global mercury cycle. *Global Biogeochem. Cycles* **2002**, *16* (4), No. 1093.

(17) Sunderland, E. M.; Mason, R. P. Human impacts on open ocean mercury concentrations. *Global Biogeochem. Cycles* **2007**, *21* (4), No. GB4022.

(18) Selin, N. E.; Jacob, D. J.; Yantosca, R. M.; Strode, S.; Jaegle, L.; Sunderland, E. M. Global 3-D land-ocean-atmosphere model for mercury: Present-day versus preindustrial cycles and anthropogenic enrichment factors for deposition. *Global Biogeochem. Cycles* **2008**, *22* (3), No. GB3099.

(19) Streets, D. G.; Devane, M. K.; Lu, Z. F.; Bond, T. C.; Sunderland, E. M.; Jacob, D. J. All-time releases of mercury to the atmosphere from human activities. *Environ. Sci. Technol.* **2011**, *45* (24), 10485–10491.

(20) Horowitz, H. M.; Jacob, D. J.; Amos, H. M.; Streets, D. G.; Sunderland, E. M. Historical mercury releases from commercial products: Global environmental implications. *Environ. Sci. Technol.* **2014**, *48* (17), 10242–10250.

(21) Amos, H. M.; Jacob, D. J.; Streets, D. G.; Sunderland, E. M. Legacy impacts of all-time anthropogenic emissions on the global mercury cycle. *Global Biogeochem. Cycles* **2013**, *27* (2), 410–421.

(22) Strode, S.; Jaegle, L.; Selin, N. E. Impact of mercury emissions from historic gold and silver mining: Global modeling. *Atmos. Environ.* **2009**, *43* (12), 2012–2017.

(23) Pirrone, N.; Allegrini, I.; Keeler, G. J.; Nriagu, J. O.; Rossmann, R.; Robbins, J. A. Historical atmospheric mercury emissions and depositions in North America compared to mercury accumulations in sedimentary records. *Atmos. Environ.* **1998**, *32* (5), 929–940.

(24) Hylander, L. D.; Meili, M. 500 years of mercury production: global annual inventory by region until 2000 and associated emissions. *Sci. Total Environ.* **2003**, *304* (1–3), 13–27.

(25) Hudson, R. J. M.; Gherini, S. A.; Fitzgerald, W. F.; Porcella, D. B. Anthropogenic influences on the global mercury cycle—A model-based analysis. *Water, Air, Soil Pollut.* **1995**, *80* (1–4), 265–272.

(26) Robins, N. A.; Hagan, N. A. Mercury production and use in colonial andean silver production: Emissions and health implications. *Environ. Health Perspect.* **2012**, *120* (5), 627–631.

(27) Camargo, J. A. Contribution of Spanish-American silver mines (1570–1820) to the present high mercury concentrations in the global environment: A review. *Chemosphere* **2002**, *48* (1), 51–57.

(28) Nriagu, J. O. Mercury pollution from the past mining of gold and silver in the Americas. *Sci. Total Environ.* **1994**, *149* (3), 167–181.

(29) Lamborg, C. H.; Hammerschmidt, C. R.; Bowman, K. L.; Swarr, G. J.; Munson, K. M.; Ohnemus, D. C.; Lam, P. J.; Heimburger, L. E.;

Rijkenberg, M. J. A.; Saito, M. A. A global ocean inventory of anthropogenic mercury based on water column measurements. *Nature* **2014**, *512* (7512), 65–+.

(30) Cooke, C. A.; Hintelmann, H.; Ague, J. J.; Burger, R.; Biester, H.; Sachs, J. P.; Engstrom, D. R. Use and Legacy of mercury in the Andes. *Environ. Sci. Technol.* **2013**, *47* (9), 4181–4188.

(31) Beal, S. A.; Jackson, B. P.; Kelly, M. A.; Stroup, J. S.; Landis, J. D. Effects of historical and modern mining on mercury deposition in Southeastern Peru. *Environ. Sci. Technol.* **2013**, *47* (22), 12715–12720.

(32) Zhang, Y.; Jaeglé, L.; Thompson, L.; Streets, D. Six centuries of changing oceanic mercury. *Global Biogeochem. Cycles* **2014**, No. 2014GB004939.

(33) Goldwater, L. *Mercury: A history of quicksilver*. York Press: Baltimore, MD, USA, 1972.

(34) Gay, D. A.; Schmeltz, D.; Prestbo, E.; Olson, M.; Sharac, T.; Tordon, R. The Atmospheric Mercury Network: measurement and initial examination of an ongoing atmospheric mercury record across North America. *Atmos. Chem. Phys.* **2013**, *13* (22), 11339–11349.

(35) GMOS. Global Mercury Observing System (GMOS): Mid-term Results, 2014.

(36) Soerensen, A. L.; Mason, R. P.; Balcom, P. H.; Sunderland, E. M. Drivers of surface ocean mercury concentrations and air–sea exchange in the west Atlantic Ocean. *Environ. Sci. Technol.* **2013**, *47* (14), 7757–7765.

(37) Lamborg, C. H.; Rolffhus, K. R.; Fitzgerald, W. F.; Kim, G. The atmospheric cycling and air–sea exchange of mercury species in the South and equatorial Atlantic Ocean. *Deep Sea Res., Part II* **1999**, *46* (5), 957–977.

(38) Temme, C.; Slemr, F.; Ebinghaus, R.; Einax, J. W. Distribution of mercury over the Atlantic Ocean in 1996 and 1999–2001. *Atmos. Environ.* **2003**, *37* (14), 1889–1897.

(39) Laurier, F. J. G.; Mason, R. P.; Whalin, L.; Kato, S. Reactive gaseous mercury formation in the North Pacific Ocean's marine boundary layer: A potential role of halogen chemistry. *J. Geophys. Res.: Atmos.* **2003**, *108* (D17), No. 12.

(40) Holmes, C. D.; Jacob, D. J.; Corbitt, E. S.; Mao, J.; Yang, X.; Talbot, R.; Slemr, F. Global atmospheric model for mercury including oxidation by bromine atoms. *Atmos. Chem. Phys.* **2010**, *10*, 12037–12057.

(41) Lyman, S. N.; Jaffe, D. A. Formation and fate of oxidized mercury in the upper troposphere and lower stratosphere. *Nat. Geosci.* **2012**, *5* (2), 114–117.

(42) Brenninkmeijer, C. A. M.; Crutzen, P.; Boumard, F.; Dauer, T.; Dix, B.; Ebinghaus, R.; Filippi, D.; Fischer, H.; Franke, H.; Friess, U.; Heintzenberg, J.; Helleis, F.; Hermann, M.; Kock, H. H.; Koepfel, C.; Lelieveld, J.; Leuenberger, M.; Martinsson, B. G.; Miemczyk, S.; Moret, H. P.; Nguyen, H. N.; Nyfeler, P.; Oram, D.; O'Sullivan, D.; Penkett, S.; Platt, U.; Pupek, M.; Ramonet, M.; Randa, B.; Reichelt, M.; Rhee, T. S.; Rohwer, J.; Rosenfeld, K.; Scharffe, D.; Schlager, H.; Schumann, U.; Slemr, F.; Sprung, D.; Stock, P.; Thaler, R.; Valentino, F.; van Velthoven, P.; Waibel, A.; Wandel, A.; Waschitschek, K.; Wiedensohler, A.; Xueref-Remy, I.; Zahn, A.; Zech, U.; Ziereis, H. Civil aircraft for the regular investigation of the atmosphere based on an instrumented container: The new CARIBIC system. *Atmos. Chem. Phys.* **2007**, *7* (18), 4953–4976.

(43) Slemr, F.; Weigelt, A.; Ebinghaus, R.; Brenninkmeijer, C.; Baker, A.; Schuck, T.; Rauthe-Schoch, A.; Riede, H.; Leedham, E.; Hermann, M.; van Velthoven, P.; Oram, D.; O'Sullivan, D.; Dyroff, C.; Zahn, A.; Ziereis, H. Mercury plumes in the global upper troposphere observed during flights with the CARIBIC Observatory from May 2005 until June 2013. *Atmosphere* **2014**, *5* (2), 342–369.

(44) Swartzendruber, P. C.; Chand, D.; Jaffe, D. A.; Smith, J.; Reidmiller, D.; Gratz, L.; Keeler, J.; Strode, S.; Jaegle, L.; Talbot, R. Vertical distribution of mercury, CO, ozone, and aerosol scattering coefficient in the Pacific Northwest during the spring 2006 INTEX-B campaign. *J. Geophys. Res.: Atmos.* **2008**, *113* (D10), No. 15.

(45) Rutter, A. P.; Schauer, J. J.; Lough, G. C.; Snyder, D. C.; Kolb, C. J.; Von Kloooster, S.; Rudolf, T.; Manolopoulos, H.; Olson, M. L. A

comparison of speciated atmospheric mercury at an urban center and an upwind rural location. *J. Environ. Monit.* **2008**, *10* (1), 102–108.

(46) Jaffe, D.; Prestbo, E.; Swartzendruber, P.; Weiss-Penzias, P.; Kato, S.; Takami, A.; Hatakeyama, S.; Kajii, Y. Export of atmospheric mercury from Asia. *Atmos. Environ.* **2005**, *39* (17), 3029–3038.

(47) Bowman, K. L.; Hammerschmidt, C. R.; Lamborg, C. H.; Swarr, G. Mercury in the North Atlantic Ocean: The U.S. GEOTRACES zonal and meridional sections. *Deep Sea Res., Part II* **2014**, in press.

(48) Mason, R. P.; Choi, A. L.; Fitzgerald, W. F.; Hammerschmidt, C. R.; Lamborg, C. H.; Soerensen, A. L.; Sunderland, E. M. Mercury biogeochemical cycling in the ocean and policy implications. *Environ. Res.* **2012**, *119*, 101–117.

(49) Smith-Downey, N. V.; Sunderland, E. M.; Jacob, D. J. Anthropogenic impacts on global storage and emissions of mercury from terrestrial soils: Insights from a new global model. *J. Geophys. Res.: Biogeosci.* **2010**, *115*, No. G03008.

(50) Grigal, D. F. Mercury sequestration in forests and peatlands: A review. *J. Environ. Qual.* **2003**, *32* (2), 393–405.

(51) Obrist, D.; Johnson, D.; Lindberg, S.; Luo, Y.; Hararuk, O.; Bracho, R.; Battles, J.; Dail, D.; Edmonds, R.; Monson, R.; Ollinger, S.; Pallardy, S.; Pregitzer, K.; Todd, D. Mercury distribution across 14 U.S. forests. Part I: Spatial patterns of concentrations in biomass, litter, and soils. *Environ. Sci. Technol.* **2011**, *45*, 3974–3981.

(52) Meili, M. The coupling of mercury and organic matter in the biogeochemical cycle—Towards a mechanistic model for the boreal forest zone. *Water, Air, Soil Pollut.* **1991**, *56*, 333–347.

(53) Potter, C. S.; Randerson, J. T.; Field, C. B.; Matson, P. A.; Vitousek, P. M.; Mooney, H. A.; Klooster, S. A. Terrestrial ecosystem production—A process model based on global satellite and surface data. *Global Biogeochem. Cycles* **1993**, *7* (4), 811–841.

(54) van der Werf, G. R.; Randerson, J. T.; Collatz, G. J.; Giglio, L. Carbon emissions from fires in tropical and subtropical ecosystems. *Global Change Biol.* **2003**, *9* (4), 547–562.

(55) van der Werf, G. R.; Randerson, J. T.; Giglio, L.; Collatz, G. J.; Kasibhatla, P. S.; Arellano, A. F. Interannual variability in global biomass burning emissions from 1997 to 2004. *Atmos. Chem. Phys.* **2006**, *6*, 3423–3441.

(56) Smith, D. B.; Cannon, W. F.; Woodruff, L. G.; Garrett, R. G.; Klassen, R.; Kilburn, J. E.; Horton, J. D.; King, H. D.; Goldhaber, M. B.; Morrison, J. M. *Major- and Trace-Element Concentrations in Soils from Two Continental-Scale Transects of the United States and Canada*, USGS Open File Report 2005-1253; U.S. Geological Survey: Reston, VA, USA, 2005.

(57) Hararuk, O.; Obrist, D.; Luo, Y. Modeling the sensitivity of soil mercury storage to climate-induced changes in soil carbon pools. *Biogeosciences* **2013**, *10*, 2393–2407.

(58) Hylander, L. D.; Meili, M. The rise and fall of mercury: Converting a resource to refuse after 500 years of mining and pollution. *Crit. Rev. Environ. Sci. Technol.* **2005**, *35* (1), 1–36.

(59) Bagnato, E.; Aiuppa, A.; Parello, F.; Allard, P.; Shinohara, H.; Liuzzo, M.; Giudice, G. New clues on the contribution of Earth's volcanism to the global mercury cycle. *Bull. Volcanol.* **2011**, *73* (5), 497–510.

(60) Bagnato, E.; Tamburello, G.; Averd, G.; Martinez-Cruz, M.; Enrico, M.; Fu, X.; Sprovieri, M.; Sonke, J. E. Mercury fluxes from volcanic and geothermal sources: An update In *Volatiles and Their Role in Petrogenetic and Eruptive Processes at Subduction Zones*, The Geological Society of London Special Publication; Zellmer, G., Edmonds, M., Straub, S., Eds.; The Geological Society of London: London, 2014; Vol. 410.

(61) Pyle, D. M.; Mather, T. A. The importance of volcanic emissions for the global atmospheric mercury cycle. *Atmos. Environ.* **2003**, *37* (36), 5115–5124.

(62) Schuster, P. F.; Krabbenhoft, D. P.; Naftz, D. L.; Cecil, L. D.; Olson, M. L.; Dewild, J. F.; Susong, D. D.; Green, J. R.; Abbott, M. L. Atmospheric mercury deposition during the last 270 years: A glacial ice core record of natural and anthropogenic sources. *Environ. Sci. Technol.* **2002**, *36* (11), 2303–2310.

(63) Lamborg, C. H.; Von Damm, K. L.; Fitzgerald, W. F.; Hammerschmidt, C. R.; Zierenberg, R. Mercury and monomethylmercury in fluids from Sea Cliff submarine hydrothermal field, Gorda Ridge. *Geophys. Res. Lett.* **2006**, *33* (17), 4.

(64) Gustin, M. S.; Lindberg, S. E.; Weisberg, P. J. An update on the natural sources and sinks of atmospheric mercury. *Appl. Geochem.* **2008**, *23* (3), 482–493.

(65) Soerensen, A. L.; Sunderland, E. M.; Holmes, C. D.; Jacob, D. J.; Yantosca, R. M.; Skov, H.; Christensen, J. H.; Strode, S. A.; Mason, R. P. An improved global model for air–sea exchange of mercury: High concentrations over the North Atlantic. *Environ. Sci. Technol.* **2010**, *44* (22), 8574–8580.

(66) Kuss, J.; Zulicke, C.; Pohl, C.; Schneider, B. Atlantic mercury emission determined from continuous analysis of the elemental mercury sea-air concentration difference within transects between 50 degrees N and 50 degrees S. *Global Biogeochem. Cycles* **2011**, *25*, No. 9.

(67) Andersson, M. E.; Sommar, J.; Gardfeldt, K.; Lindqvist, O. Enhanced concentrations of dissolved gaseous mercury in the surface waters of the Arctic Ocean. *Mar. Chem.* **2008**, *110* (3–4), 190–194.

(68) Soerensen, A. L.; Mason, R. P.; Balcom, P. H.; Jacob, D. J.; Zhang, Y.; Kuss, J.; Sunderland, E. M. Elemental mercury concentrations and fluxes in the tropical atmosphere and ocean. *Environ. Sci. Technol.* **2014**, *48* (19), 11312–11319.

(69) Tseng, C. M.; Lamborg, C. H.; Hsu, S. C. A unique seasonal pattern in dissolved elemental mercury in the South China Sea, a tropical and monsoon-dominated marginal sea. *Geophys. Res. Lett.* **2013**, *40* (1), 167–172.

(70) Andersson, M. E.; Gardfeldt, K.; Wangberg, I.; Sprovieri, F.; Pirrone, N.; Lindqvist, O. Seasonal and daily variation of mercury evasion at coastal and off shore sites from the Mediterranean Sea. *Mar. Chem.* **2007**, *104* (3–4), 214–226.

(71) Fantozzi, L.; Ferrara, R.; Frontini, F. P.; Dini, F. Factors influencing the daily behaviour of dissolved gaseous mercury concentration in the Mediterranean Sea. *Mar. Chem.* **2007**, *107* (1), 4–12.

(72) Bagnato, E.; Sproveri, M.; Barra, M.; Bitetto, M.; Bonsignore, M.; Calabrese, S.; Di Stefano, V.; Oliveri, E.; Parello, F.; Mazzola, S. The sea-air exchange of mercury (Hg) in the marine boundary layer of the Augusta basin (southern Italy): Concentrations and evasion flux. *Chemosphere* **2013**, *93* (9), 2024–2032.

(73) Whalin, L.; Kim, E. H.; Mason, R. Factors influencing the oxidation, reduction, methylation and demethylation of mercury species in coastal waters. *Mar. Chem.* **2007**, *107* (3), 278–294.

(74) Rolffhus, K. R.; Fitzgerald, W. F. Mechanisms and temporal variability of dissolved gaseous mercury production in coastal seawater. *Mar. Chem.* **2004**, *90* (1–4), 125–136.

(75) Amyot, M.; Gill, G. A.; Morel, F. M. M. Production and loss of dissolved gaseous mercury in coastal seawater. *Environ. Sci. Technol.* **1997**, *31* (12), 3606–3611.

(76) Qureshi, A.; O'Driscoll, N. J.; MacLeod, M.; Neuhold, Y. M.; Hungerbuhler, K. Photoreactions of mercury in surface ocean water: Gross reaction kinetics and possible pathways. *Environ. Sci. Technol.* **2010**, *44* (2), 644–649.

(77) Lalonde, J. D.; Amyot, M.; Kraepiel, A. M. L.; Morel, F. M. M. Photooxidation of Hg(0) in artificial and natural waters. *Environ. Sci. Technol.* **2001**, *35* (7), 1367–1372.

(78) Carpi, A.; Lindberg, S. E. Sunlight-mediated emission of elemental mercury from soil amended with municipal sewage sludge. *Environ. Sci. Technol.* **1997**, *31* (7), 2085–2091.

(79) Allard, B.; Arsenie, I. Abiotic reduction of mercury by humic substances in aquatic system—An important process for the mercury cycle. *Water, Air, Soil Pollut.* **1991**, *56*, 457–464.

(80) Amyot, M.; Mierle, G.; Lean, D. R. S.; McQueen, D. J. Sunlight-induced formation of dissolved gaseous mercury in lake waters. *Environ. Sci. Technol.* **1994**, *28* (13), 2366–2371.

(81) Hines, N. A.; Brezonik, P. L. Mercury dynamics in a small Northern Minnesota lake: Water to air exchange and photoreactions of mercury. *Mar. Chem.* **2004**, *90* (1–4), 137–149.

- (82) Hines, N. A.; Brezonik, P. L. Mercury inputs and outputs at a small lake in northern Minnesota. *Biogeochemistry* **2007**, *84* (3), 265–284.
- (83) Graydon, J. A.; St. Louis, V. L.; Lindberg, S. E.; Sandilands, K. A.; Rudd, J. W. M.; Kelly, C. A.; Harris, R.; Tate, M. T.; Krabbenhoft, D. P.; Emmerton, C. A.; Asmath, H.; Richardson, M. The role of terrestrial vegetation in atmospheric Hg deposition: Pools and fluxes of spike and ambient Hg from the METAALICUS experiment. *Global Biogeochem. Cycles* **2012**, 2610.1029/2011GB004031.
- (84) Obrist, D.; Pokharel, A. K.; Moore, C. Vertical profile measurements of soil air suggest immobilization of gaseous elemental mercury in mineral soil. *Environ. Sci. Technol.* **2014**, *48* (4), 2242–2252.
- (85) Cossa, D.; Coquery, M.; Gobeil, C.; Martin, J. M. Mercury fluxes at the ocean margins. In *Global and Regional Mercury Cycles: Sources, Fluxes and Mass Balances*; Baeyens, W., Ebinghaus, R.; Vasiliev, O., Eds.; Springer: Dordrecht, The Netherlands, 1996; Vol. 21, pp 229–247.
- (86) Chester, R., The transport of material to the oceans: Relative flux magnitudes. In *Marine Geochemistry*, 2nd ed.; Chester, R., Ed.; Blackwell Science: Oxford, U.K., 2003; pp 98–134.
- (87) Mason, R. P.; Lawrence, A. L. Concentration, distribution, and bioavailability of mercury and methylmercury in sediments of Baltimore Harbor and Chesapeake Bay, Maryland, USA. *Environ. Toxicol. Chem.* **1999**, *18* (11), 2438–2447.
- (88) Balcom, P. H.; Hammerschmidt, C. R.; Fitzgerald, W. F.; Lamborg, C. H.; O'Connor, J. S. Seasonal distributions and cycling of mercury and methylmercury in the waters of New York/New Jersey harbor estuary. *Mar. Chem.* **2008**, *109* (1–2), 1–17.
- (89) Balcom, P. H.; Fitzgerald, W. F.; Vandal, G. M.; Lamborg, C. H.; Rolffus, K. R.; Langer, C. S.; Hammerschmidt, C. R. Mercury sources and cycling in the Connecticut River and Long Island Sound. *Mar. Chem.* **2004**, *90* (1–4), 53–74.
- (90) Sunderland, E. M.; Dalziel, J.; Heyes, A.; Branfireun, B. A.; Krabbenhoft, D. P.; Gobas, F. Response of a macrotidal estuary to changes in anthropogenic mercury loading between 1850 and 2000. *Environ. Sci. Technol.* **2010**, *44* (5), 1698–1704.
- (91) Macleod, M.; McKone, T. E.; Mackay, D. Mass balance for mercury in the San Francisco Bay Area. *Environ. Sci. Technol.* **2005**, *39* (17), 6721–6729.
- (92) Balcom, P. H.; Fitzgerald, W. F.; Mason, R. P. *Synthesis and Assessment of Heavy Metal Contamination in the Hudson River and New York/New Jersey Harbor Estuary*; Hudson River Foundation: New York, 2010.
- (93) Hammerschmidt, C. R.; Fitzgerald, W. F. Methylmercury cycling in sediments on the continental shelf of southern New England. *Geochim. Cosmochim. Acta* **2006**, *70* (4), 918–930.
- (94) Harris, R.; Pollman, C.; Hutchinson, D.; Landing, W.; Axelrad, D.; Morey, S. L.; Dukhovskoy, D.; Vijayaraghavan, K. A screening model analysis of mercury sources, fate and bioaccumulation in the Gulf of Mexico. *Environ. Res.* **2012**, *119*, 53–63.
- (95) Hollweg, T. A.; Gilmour, C. C.; Mason, R. P. Mercury and methylmercury cycling in sediments of the mid-Atlantic continental shelf and slope. *Limnol. Oceanogr.* **2010**, *55* (6), 2703–2722.
- (96) Shotyk, W.; Goodsite, M. E.; Roos-Barraclough, F.; Frei, R.; Heinemeier, J.; Asmund, G.; Lohse, C.; Hansen, T. S. Anthropogenic contributions to atmospheric Hg, Pb and As accumulation recorded by peat cores from southern Greenland and Denmark dated using the ^{14}C "bomb pulse curve". *Geochim. Cosmochim. Acta* **2003**, *67* (21), 3991–4011.
- (97) Nriagu, J. O.; Wong, H. K. T.; Lawson, G.; Daniel, P. Saturation of ecosystems with toxic metals in Sudbury basin, Ontario, Canada. *Sci. Total Environ.* **1998**, *223* (2–3), 99–117.
- (98) Munthe, J.; Hultberg, H. Mercury and methylmercury in runoff from a forested catchment—Concentrations, fluxes, and their response to manipulations. *Water, Air, Soil Pollut.: Focus* **2004**, *4* (2–3), 607–618.
- (99) Cooke, C. A.; Hobbs, W. O.; Michelutti, N.; Wolfe, A. P. Reliance on Pb-210 chronology can compromise the inference of preindustrial Hg flux to lake sediments. *Environ. Sci. Technol.* **2010**, *44* (6), 1998–2003.
- (100) Abril, J. M.; Brunskill, G. J. Evidence that excess Pb-210 flux varies with sediment accumulation rate and implications for dating recent sediments. *J. Paleolimnol.* **2014**, *52* (3), 121–137.
- (101) Baskaran, M.; Nix, J.; Kuyper, C.; Karunakara, N. Problems with the dating of sediment core using excess Pb-210 in a freshwater system impacted by large scale watershed changes. *J. Environ. Radioact.* **2014**, *138*, 355–363.
- (102) Smith, J. N. Why should we believe Pb-210 sediment geochronologies? *J. Environ. Radioact.* **2001**, *55* (2), 121–123.
- (103) Hancock, G.; Edgington, D. N.; Robbins, J. A.; Smith, J. N.; Brunskill, G.; Pfitzner, K. Workshop on radiological techniques in sedimentation studies: Methods and applications. In *Proceedings of the South Pacific Environmental Radioactivity Association*, Paris; Fernandez, J. M., Fiches, R., Eds.; IRD Editions: Paris, France, **2002**; p 423.
- (104) Lacerda, L. D. Global mercury emissions from gold and silver mining. *Water, Air, Soil Pollut.* **1997**, *97* (3–4), 209–221.
- (105) Robins, N. *Mercury, mining, and empire: The human and ecological costs of colonial silver mining in the Andes*; Indiana University Press: Bloomington, IN, USA, 2011.
- (106) Guerrero, S. Chemistry as a tool for historical research: Identifying paths of historical mercury pollution in the Hispanic New World. *Bull. Hist. Chem.* **2012**, *37* (2), 61–70.
- (107) Hagan, N.; Robins, N.; Hsu-Kim, H.; Halabi, S.; Morris, M.; Woodall, G.; Zhang, T.; Bacon, A.; Richter, D. D.; Vandenberg, J. Estimating historical atmospheric mercury concentrations from silver mining and their legacies in present-day surface soil in Potosi, Bolivia. *Atmos. Environ.* **2011**, *45* (40), 7619–7626.
- (108) Nriagu, J. O. Legacy of mercury pollution. *Nature* **1993**, *363* (6430), 589–589.
- (109) Cooke, C. A.; Balcom, P. H.; Kerfoot, C.; Abbott, M. B.; Wolfe, A. P. Pre-Colombian mercury pollution associated with the smelting of Argentiferous ores in the Bolivian Andes. *Ambio* **2011**, *40* (1), 18–25.
- (110) Kim, C. S.; Rytuba, J. J.; Brown, G. E., Jr. Geological and anthropogenic factors influencing mercury speciation in mine wastes: An EXAFS spectroscopy study. *Appl. Geochem.* **2004**, *19* (3), 379–393.
- (111) Gray, J. E.; Crock, J. G.; Fey, D. L. Environmental geochemistry of abandoned mercury mines in West-Central Nevada, USA. *Appl. Geochem.* **2002**, *17* (8), 1069–1079.
- (112) Maramba, N. P. C.; Reyes, J. P.; Francisco-Rivera, A. T.; Panganiban, L. C. R.; Dioquino, C.; Dando, N.; Timbang, R.; Akagi, H.; Castillo, M. T.; Quitoriano, C.; Afuang, M.; Matsuyama, A.; Eguchi, T.; Fuchigami, Y. Environmental and human exposure assessment monitoring of communities near an abandoned mercury mine in the Philippines: A toxic legacy. *J. Environ. Manage.* **2006**, *81* (2), 135–145.
- (113) Boutron, C. F.; Vandal, G. M.; Fitzgerald, W. F.; Ferrari, C. P. A forty year record of mercury in central Greenland snow. *Geophys. Res. Lett.* **1998**, *25* (17), 3315–3318.
- (114) Obrist, D.; Johnson, D. W.; Lindberg, S. E.; Luo, Y.; Hararuk, O.; Bracho, R.; Battles, J. J.; Dail, D. B.; Edmonds, R. L.; Monson, R. K.; Ollinger, S. V.; Pallardy, S. G.; Pregitzer, K. S.; Todd, D. E. Mercury distribution across 14 U.S. forests. Part I: Spatial patterns of concentrations in biomass, litter, and soils. *Environ. Sci. Technol.* **2011**, *45* (9), 3974–3981.
- (115) Eckley, C. S.; Parsons, M. T.; Mintz, R.; Lapalme, M.; Mazur, M.; Tordon, R.; Elleman, R.; Graydon, J. A.; Blanchard, P.; St. Louis, V. Impact of closing Canada's largest point-source of mercury emissions on local atmospheric mercury concentrations. *Environ. Sci. Technol.* **2013**, *47* (18), 10339–10348.
- (116) Iverfeldt, A.; Munthe, J.; Brosset, C.; Pacyna, J. Long-term changes in concentration and deposition of atmospheric mercury over Scandinavia. *Water, Air, Soil Pollut.* **1995**, *80* (1–4), 227–233.
- (117) Mather, T. A.; Witt, M. L. I.; Pyle, D. M.; Quayle, B. M.; Aiuppa, A.; Bagnato, E.; Martin, R. S.; Sims, K. W. W.; Edmonds, M.; Sutton, A. J.; Ilyinskaya, E. Halogens and trace metal emissions from

the ongoing 2008 summit eruption of Kilauea volcano, Hawaii. *Geochim. Cosmochim. Acta* **2012**, *83*, 292–323.

(118) Varekamp, J. C.; Buseck, P. R. Global mercury flux from volcanic and geothermal sources. *Appl. Geochem.* **1986**, *1* (1), 65–73.

(119) Wilson, S.; Munthe, K.; Sundseth, K.; Kindbom, K.; Maxson, P.; Pacyna, P.; Steenhuisen, F. *Updating historical global inventories of anthropogenic mercury emissions to air*; Arctic Monitoring and Assessment Programme (AMAP): Oslo, Norway, 2010; p 14.

(120) Pacyna, E. G.; Pacyna, J. M.; Sundseth, K.; Munthe, J.; Kindbom, K.; Wilson, S.; Steenhuisen, F.; Maxson, P. Global emission of mercury to the atmosphere from anthropogenic sources in 2005 and projections to 2020. *Atmos. Environ.* **2010**, *44* (20), 2487–2499.

(121) Muntean, M.; Janssens-Maenhout, G.; Song, S. J.; Selin, N. E.; Olivier, J. G. J.; Guizzardi, D.; Maas, R.; Dentener, F. Trend analysis from 1970 to 2008 and model evaluation of EDGARv4 global gridded anthropogenic mercury emissions. *Sci. Total Environ.* **2014**, *494*, 337–350.

(122) AMAP/UNEP. *Technical Background Report for the Global Mercury Assessment 2013*; Arctic Monitoring and Assessment Program (AMAP)/UNEP Chemicals Branch: Oslo, Norway/Geneva, Switzerland, 2013; p vi + 263 pp.

(123) Rafaj, P.; Bertok, I.; Cofala, J.; Schöpp, W. Scenarios of global mercury emissions from anthropogenic sources. *Atmos. Environ.* **2013**, *79* (0), 472–479.

(124) Li, P.; Feng, X. B.; Qiu, G. L.; Li, Z. G.; Fu, X. W.; Sakamoto, M. S.; Liu, X. J.; Wang, D. Y. Mercury exposures and symptoms in smelting workers of artisanal mercury mines in Wuchuan, Guizhou, China. *Environ. Res.* **2008**, *107* (1), 108–114.

(125) Maxson, P. *Mercury Flows in Europe and the World: Impact of Decommissioned Chlor-alkali Plants*; European Commission, Directorate General for Environment: Brussels, Belgium, 2004; p 104.